이학석사 학위논문

Activity-dependent modulation of synaptic vesicle retrieval mechanisms at CNS synapses

중추신경에서 신경세포 활성에 따른 시냅스낭 이입 과정의 조절에 관한 연구

2016년 08월

서울대학교 대학원

뇌과학 협동과정

조 오 연

ABSTRACT

Activity-dependent modulation of synaptic vesicle retrieval mechanisms at CNS synapses

Oh Yeon Cho

Interdisciplinary Program in Neuroscience

The Graduate School

Seoul National University

Typical central synapses contain a limited number of synaptic vesicles (SVs). To continuously release neurotransmitters in response to repetitive stimulation, the SVs need to be quickly replenished through endocytosis and recycling. Previous studies proposed that SV retrieval occurs exclusively via clathrin-mediated endocytosis (CME). Recently however, some reports have challenged this view and suggested that clathrin-independent

endocytosis (CIE) via either ultrafast endocytosis or bulk endocytosis is functional instead. In this study, I examined how neurons use CME and CIE depending on different neuronal activity in primary cultured hippocampal neurons since neuronal activity may modulate the mode of SVs retrieval. I found that during low-frequency stimulation at 5 Hz, SVs were retrieved mostly via CME. Accordingly, inhibition of CIE by Brefeldin A (BFA) treatment or adaptor protein (AP)-1/AP-3 Knockdown (KD) did not affect SV retrieval during 5 Hz stimulation. However, when CME was blocked via clathrin heavy chain (CHC) KD or PITSTOP 2 treatment, which is an inhibitor between amphiphysin and clathrin, SVs initially underwent endocytosis for approximately 10 s of stimulation, after which time CIE became operative and compensated for the deficiency of CME. Moreover, endocytosis after stimulation was not affected by CIE inhibition whereas CME inhibition resulted in a slow rate of endocytosis. In contrast, during high frequency stimulation at 40 Hz, I found that after a brief delay, SVs were retrieved exclusively by CIE since the blockage of CIE completely abolished the endocytosis during stimulation while CME inhibition did not affect during-stimulus endocytosis. Post-stimulus endocytosis also was not affected by CME inhibition while CIE blockage slowed the rate of post-stimulus endocytosis. These results show that mature neurons use CME and CIE pathways to different extents depending on neuronal activity to retrieve SVs during stimulation. When either one pathway is blocked, the other pathway can compensate for the deficiency. This may result in activity-dependent alteration of the SVs retrieval, which ultimately influences the efficiency of neurotransmitter release and contributes to synaptic plasticity.

Keywords **:** neuronal activity, CME, CIE, synaptic vesicle retrieval, Activity-dependent modulation

Student Number **: 2014-22453**

CONTENTS

LIST OF FIGURES

Figure 9. **Deficiency of CIE slows endocytosis at high-frequency stimulation.**

LIST OF ABBREVIATIONS

CNS, Central nerves system

SVs, Synaptic vesicles

CME, Clathrin-mediated endocytosis

CIE, Clathrin independent endocytosis

BFA, Brefeldin A

AP-1, Adaptor protein 1

AP-3, Adaptor protein 3

KD, Knockdown

CHC, Clathrin heavy chain

shRNA, Small hairpin RNA

Foli, Folimycin

DIV, Days in vitro

vGpH, vesicular glutamate transporter 1-pHluorin

APs, Action potentials

Introduction

In the central nervous system (CNS), communication between neurons mainly occurs at synapses. At the chemical synapse, electrical signals controlled neurotransmitter release by exocytosis of synaptic vesicles (SVs) at the presynaptic neurons. The fusion of SVs releases neurotransmitters that diffuse across the synaptic cleft and transmit the signal to post-synaptic neurons [1, 2]. Retained the number of SVs in a presynaptic terminal, fusion of many SVs would result in fast depletion of SVs then lead to loss of function to communicate between pre- and post- synapses. Furthermore, the continuous fusion of SVs in the absence of compensatory membrane retrieval would increase the area of the presynaptic plasma membrane. Therefore, to back up rapid and repeated SVs release, the presynaptic membrane retrieval is required to maintain synaptic function during sustained synaptic activities [3]. Although many research has led to a deep understanding of the specific property of SVs to undergo recycling [4, 5], the precise mechanisms about which endocytic ways are dominant to recycling SVs and what could be modulated this SVs retrieval is still enigmatic.

SVs reformation involves both retrieval of SVs components from the plasma membrane, and the regeneration of functional SVs. Particularly, the mechanism of the membrane retrieval has drawn the attention to the researchers because of synaptic transmission gravity. Among the decades of researches, three different retrieval

pathways have been proposed. *Kiss-and-run* pathway enables the SVs retrieved within one second without full fusion [6-8]. Other two retrieval pathways of SVs membrane pathways are retrieval after full fusion from plasma membrane; Clathrin-mediated endocytosis (CME), and clathrin-independent bulk endocytosis (CIE). In CME, a SV is generated from the plasma membrane with a time constant of about 10 s using clathrin, adaptor protein-2 (AP-2) and many accessory proteins. Unlike CME, CIE is observed during heavy stimulation when large membrane infoldings appear which lead to the generation of large endosomal-like vacuoles. Then, SVs bud out from these endosome-like vacuoles via AP-1 and AP-3 dependent mechanisms [9, 10].

Despite tremendous progresses for many years, many aspects of this topic still remain unclear, which include which SVs retrieval pathway is going to be dominant and what may modulate the pathway of SVs retrieval. Although CME has been known as a dominant mechanism of SVs retrieval, recent data showed that depletion of clathrin results in the inhibition of fission from endosome-like vacuoles and lead to decrease of SVs number. In contrast, SVs membrane retrieval from plasma membrane was unaffected, in particular during high-frequency stimulation. Clathrin and AP-2 mediate SVs formation from endocytosed endosomal structures, suggesting stimulation-dependent modulation of endocytic mechanisms at CNS synapses [12].

Recently, another membrane retrieval pathway called ultrafast endocytosis has been reported. Ultrafast endocytosis retrieves single, large endocytic vesicles directly

adjacent to presynaptic densities as fast as 50~100 ms after SVs fusion in response to a single stimulus or during mild stimulation [13]. Clathrin is not required for ultrafast endocytosis but is required to generate SVs from the endosomes at physiological temperature. While, at room temperature, CME functions at the plasma membrane [14]. Therefore, the frequency of stimulation or temperature could be the regulating factor that determines whether the CME and CIE pathway is used.

As neuronal activity may modulate the mode of SV retrieval, I examined how neurons use CME and CIE according to the neuronal activity in primary cultured hippocampal neurons. From my analysis, SVs are retrieved mostly via CME when stimulation is at low-frequency (5 Hz). At the same time, the inhibition of CIE by BFA treatment or AP-1/AP-3 KD did not affect the performance of the SV retrieval. Further examination showed that when CME was suppressed by clathrin heavy chain (CHC) KD or PITSTOP 2 treatment, SV endocytosis was initially halted for about 10 s. However, this deficiency of CME was compensated later on by CIE. While CIE inhibition did not affect the endocytosis after stimulation, the CME inhibition resulted slowness in the process. In contrast, at high-frequency stimulation (40 Hz), I noticed that SVs were retrieved solely by CIE after a brief delay. During the stimulation, the CIE blockage completely abolished the endocytosis while the CME inhibition did not affect the during-stimulus endocytosis. CIE blockage slowed post-stimulus endocytosis but the CME inhibition still remained to be effectless to the endocytosis. My results provided that mature neurons use CME and CIE pathway different extents, depending

on the neuronal activity in retrieving SVs during stimulation. When either one pathway is blocked, the other pathway can compensate for the deficiency and may lead to activity-dependent alterations of the SV retrieval's efficiency. This ultimately influences the efficient of transmitter to release and contribute to synaptic plasticity.

Material and Method

A. DNA constructs

The shRNA for AP-1, AP-3 or CHC were designed from the following oligonucleotides: AP-1 (γ subunit, rat), 5'-GCGCCTGTACAAGGCAATT-3'; AP-3 (δ subunit, rat), 5'-ACAAAGTGTTCCTCAAGTA-3', CHC (rat), 5'-GTCGCCCTTCTGAAGGTCCT-3'. Complementary oligonucleotides were synthesized separately, and carried out by expressing paired shRNA through a pSIREN-DNR-DsRed vector. After transfection, the neurons were incubated for more than 5 days for pHluorin assay. The accuracy of all constructs was verified by DNA sequencing. vGlut1-pHluorin (vGpH) was kindly provided by Dr. John Rubenstein at University of California-San Francisco.

B. Materials

Folimycin (*Foli*) was from Calbiochem (San Diego, CA) while Brefeldin A (BFA) was from Cell Signaling Technology (Boston, MA). 6-cyano-7-nitroquinoxaline-2, 3-dione (CNQX) were from Tocris Bioscience (Bristol, UK) and Dimethyl sulfoxide (DMSO) and other chemicals were from Sigma (St. Louis, MO).

C. Neuron culture and transfection

Hippocampal neurons derived from embryonic day 18 Sprague Dawley fetal rats were prepared as described [15]. Hippocampal DG–CA3 regions of embryonic hippocampi were dissected, dissociated with papain, and triturated with a polished half-bore Pasteur pipette. Dissociated cells (2.5×10^5) in Hank's Balanced Salt Solution (HBSS, HyClone) supplemented with 0.6 % glucose, 1 mM pyruvate, 2 mM L-glutamine, and 10 % (v/v) FBS (HyClone). Then those cells plated on Poly-D-lysine-coated glass coverslips in a 60-mm Petri dish. Four hours after plating, the medium was replaced with Neurobasal media (Invitrogen) supplemented with 2 % (v/v) NS21 and 0.5 mM L-glutamine. Neuronal cultures were kept in an incubator at 37 ℃ and 5 % CO_2 before use. Cultured Neurons were transfected using a modified calcium-phosphate method [16] at DIV 9. In short, total 6 μg of cDNA and 9.3 μl of 2 M $CaCl_2$ was mixed in distilled water to a total volume of 75 μl, and same volume of 2X N, N-bis[2-hydroxyethyl]-2-aminoethanesulfonic acid-buffered saline was added. The cell culture medium was completely replaced by transfection medium (MEM, 1 mM pyruvate, 0.6 % glucose, 10 mM glutamine, and 10 mM N-2-hydroxyl piperazine-N'-2-ethane sulfonic acid (HEPES), pH 7.65). The cDNA mixture was added to the neurons, and incubated in a 5 % CO_2 incubator for 1 hour. Neurons were washed twice with washing medium (pH 7.35) for 30 min and then returned to the original culture medium. The vGpH and pSIREN-empty or shRNA constructs were cotransfected in a ratio of 1:2. Neurons were cotransfected at DIV 9 and used at between DIV 14 and 16.

D. vGlut1-pHluorin exo/endocytosis assay and Image Analysis

Neurons with vGpH transfection were mounted in a perfusion/stimulation chamber, and equipped with platinum-iridium field stimulus electrodes (Chamlide EC, LCI, Korea) on the stage of an Olympus IX-71, which inverted microscope with 60 X, 1.35 NA oil lens (Olympus, Tokyo, Japan). The cells were continuously perfused at 34 °C temperature with Tyrode solution containing the following: 136 mM NaCl, 2.5 mM KCl, 2 mM $CaCl_2$, 1.3mM $MgCl_2$, 10 mM HEPES, and 10 mM D-glucose, pH 7.3. Temperature was controlled by a heating controller system (LCI, Korea) about chamber and lens. 10 μM 6-cyano-7-nitroquinoxaline-2,3-dione (CNQX) and 50 μM of DL-2-amino-5-phosphonovaleric acid (AP-V) were added to Imaging buffer to reduce spontaneous activity and to prevent recurrent excitation during stimulation. Time-lapse images were acquired in every 500 ms or 2 s for 2 min using a Zyla 5.5 sCMOS camera (Andor Technologies, Belfast, Northern Ireland) driven by MetaMorph Imaging software (Molecular Devices, Sunnyvale, CA). From the 4^{th} frame, the neurons were stimulated (1 ms, 30-50 V, bipolar) using an A310 Accupulser current stimulator (World Precision Instruments, Sarasota, FL).

Quantitative measurements of the fluorescence intensity at individual boutons were obtained by averaging a selected area of pixel intensities using Image J (NIH). We

selected the ROI (Region of Interest) following this rules by hand using Image J and average intensities were calculated. Large puncta, typically representative of clusters of smaller synapses, were rejected during the selection procedure. The center of intensity of each synapse was calculated to correct for any image shifts over the course of the experiment. Fluorescence was expressed in intensity units that correspond to fluorescence values averaged over all pixels within the region-of-interest. All fitting was done using individual error bars to weight the fit, using Origin Pro 9.0 (OriginLab Corporation, Northampton, MA). To obtain the endocytic time constant after stimulation, the decay of vGpH after stimulation was fitted with double exponential function. In some experiments in which fluorescence decay does not down to zero at the time constant was obtained using the initial slope method. In this method, a line is drawn from the initial point at the initial slope and where that line intersects the final value is the time constant. For exocytosis assays, neurons were pre-incubated with *Foli* for 20 s to block the reacidification and stimulated as same as first train. Net fluorescence changes were obtained by subtracting the average intensity of the first four frames (F_0) from the intensity of each frame (F_t) for individual boutons, normalizing to the maximum fluorescence intensity (F_{max} - F_0), and then averaging. To get endocytic rate during stimulation, neurons were stimulated in the presence or absence of *Foli*. In the absence of *Foli*, the fluorescence signal reflects the net balance of exocytosis and endocytosis ($\Delta F_{exo-endo}$). In the presence of *Foli*, exocytosis events are trapped in an alkaline state and the fluorescence signal reflects exocytosis (ΔF_{exo}). Fluorescence

values were normalized to the peak fluorescence in each experimental condition. Endocytosis during stimulation was derived by subtracting the vGpH fluorescence in the absence of *Foli* from that in the presence of *Foli* ($\Delta F_{endo} = \Delta F_{exo} - \Delta F_{exo-endo}$). The traces were normalized to the maximum stable fluorescence signal after *Foli* treatment. Rate of exocytosis and rate of endocytosis were obtained from the linear fits to the data during a 200 APs stimulus during stimulation. Photo-bleaching drift was corrected empirically using either local background or time-lapse imaging without stimulation before the experiments. Because both yielded similar results, we only used the local background method throughout the study. We selected the regions where blurred fluorescence signals are observed, and those where no active changes in fluorescence intensity were observed during experiments. We took decay kinetics of these local backgrounds by fitting double exponential function to local background decay signal and then subtracting this function from the original trace. The result was a trace with a relatively flat baseline. Data were collected from 50 boutons of 12–24 neurons in each coverslip. Statistical analysis was performed with SigmaPlot version 10.0 for using unpaired *student's* T-test, and SPSS version 21. For multiple conditions, we compared the means by ANOVA followed by Fisher's LSD test (depending on the number of groups). Significant differences were accepted at $p < 0.05$.

E. Drug treatment

BFA or PITSTOP 2 were prepared as 10 mg/ml or 25 mM stock solutions in 100 % DMSO, respectively, and stored at −20 °C. Drugs were diluted directly into the Tyrode solution; final DMSO concentration was 0.1 % (v/v). Neurons were incubated with 10 μg/ml BFA or 25 μM PITSTOP 2 for 30 min at 37 °C. The neurons transfected with vGpH were acquired time-lapse images, which were stimulated at 5 Hz or 40 Hz, 200 APs. During imaging, BFA or PITSTOP 2 was included in the Tyrode solution. For exocytosis assay, neurons were acquired time-lapse images, which were stimulated as the same as before with *Foli* and each drugs. Also neurons were incubated and stimulated with 0.1 % DMSO vehicle for control of drug treatment.

Results

SVs membrane retrieval is modulated by stimulation frequency

In a physiological condition, mammalian CNS neurons can respond to a broad range of physiological stimulation patterns ranging from a few to tens of hertz (Hz). One possible reason for the apparent discrepancies between various studies on SVs recycling is that the mode of presynaptic membrane retrieval may depend on the frequency of stimulation. To probe how stimulation frequency affects SVs membrane retrieval in hippocampal neurons, I used the pH-sensitive GFP (pHluorin) fused to vesicular glutamate transporter-1 (vGlut-1). pHluorins undergo quenching inside the SVs lumen because of acidic environment and are dequenched upon exposure to neutral pH of 7.4 during exocytosis [17]. Because of pH-sensitive change in fluorescence intensities, vGlut1-pHluorin (vGpH) is suitable reporter to monitor SVs exo/endocytosis and subsequent reacidification [11, 18]. Cultured hippocampal neurons were stimulated at the identical numbers of action potentials (200 APs) applied at either low- (5 Hz) or high- (40 Hz) frequency, respectively. To examine how frequency modulates SV retrieval between endocytosis and exocytosis, I applied the H^+-ATPase inhibitor folimycin (*Foli*) (Fig. 1 A1-2). *Foli* can prevent reacidification after SV retrieval, thereby allowing to measure pure exocytosis quantitatively during stimulation [18]. Compared to neurons with 40 Hz stimulation, neurons at 5 Hz stimulus exhibited a

decrease in the rate of vGpH release and retrieval kinetics (Fig. 1 B1-2). To distinguish between exocytosis and endocytosis, I measured the slope of exo/endocytosis that indicated the rate of exo/endocytosis respectively. Rate of exo/endocytosis during stimulation were obtained from the linear fit. At the first glance, slope value of during-stimulus endocytosis was increased at 40 Hz in comparison to stimulate at 5 Hz (Fig. 1 C1-2, 4). However, slope value of exocytosis, when stimulated at 40 Hz, was also increased more than three times compared to 5 Hz (Fig. 1 C1-2, 3). In addition, when applied at the high-frequency stimulation, there is barely retrieved SVs after a brief delay. Then, I calculated the ratio of endo/exocytosis to compare during-stimulus endocytosis at 5 Hz and 40 Hz. The ratio of endo/exocytosis at 5 Hz frequency stimulation is twice higher than ratio at 40 Hz stimulation (Fig. 1 C5). However, post-stimulus endocytosis is not affected by frequency of stimulation. (Fig. 1 D; τ_{5Hz}=15.79 ± 1.38 s and τ_{40Hz}=10.82 ± 1.20 s). Taken together all the result, stimulation frequency is a modulator of SVs membrane retrieval.

Blockage of CME by using PITSTOP 2 lead to during- and post- stimulus endocytic defect at low-frequency stimulation

The distinction of endocytosis rate between low- and high-frequency stimulation could conceive two scenarios: 1) reflect a single mode of SVs endocytosis running through distinct kinetic bottlenecks or 2) different endocytic modes operating in parallel.

In a previous study, SVs retrieval occurring exclusively via CME has been proposed. Following this proposal, I carried out PITSTOP 2 pre-treatment to hippocampal neurons after cotransfection with vGpH and pSIREN-empty to inhibit CME. PITSTOP 2 is an inhibitor of interaction between amphiphysin and clathrin, thus it inhibits CME (25 μM) [19]. Each synapses stimulated with 200 APs applied at 5 Hz (Fig. 2 A1-2). Unlike control neurons treated with 0.1 % DMSO, synapses of PITSTOP 2 treated neurons showed stopped during-stimulus endocytosis until ~ 10 s, but later on resumed with the comparable endocytic rate with control. The rate of exocytosis was nearly same (Fig. 2 B1-5; endocytic rate: 0.009 ± 0.0007 for the control, 0.002 ± 0.0010 for the PITSTOP 2 treated until ~ 10 s, and 0.0115 ± 0.0013 for the PITSTOP 2 treated after 10 s, exocytic rate: 0.0239 ± 0.0001 for the control, 0.0243 ± 0.0003 for the PITSTOP 2 treated). PITSTOP 2 treated neurons also showed a significant slowdown of the post-stimulus endocytosis (Fig. 2 C; $\tau_{control}$=11.35 ± 1.06 s, $\tau_{PITSTOP2}$=21.45 ± 0.98 s). The data showed that when CME is pharmacologically blocked, during-stimulus endocytosis was halted for few seconds but resumed later on. In addition, post-stimulus retrieval kinetics were slowed and vesicles were not retrieved entirely. These data indicated that when CME is blocked, CIE could contribute to compensatory membrane retrieval at hippocampal synapses with 5 Hz stimulation. Moreover, post-stimulus membrane retrieval by CIE was slower than retrieval by both endocytic modes; CME and CIE.

Deletion of endogenous Clathrin by shRNA also lead to during- and post- stimulus endocytic defect at low-frequency stimulation same as PITSTOP 2

Recently, it has been proposed that PITSTOP 2 could inhibit CIE as well [20]. To avoid the side effect of PITSTOP 2 and confirm these surprising results, I depleted endogenous CHC using small hairpin RNA (shRNA). The target shRNA sequences was conformed as published before. These target sequences have been shown to lead to strong reduction of endogenous clathrin level to about ~30 % [12]. Clathrin depleted synapses and synapses that expressed scrambled sequences, as a control, were stimulated with identical stimulation as above to measure the rate of SVs membrane retrieval (Fig 3 A1-2). The CHC knockdown synapses showed that during-stimulus endocytosis was halted in early phase, and the later phase followed the rate of control synapses endocytosis. The exocytosis was nearly same (Fig. 3 B1-5; endocytic rate: 0.0113 ± 0.0007 for the 5 Hz, 0.0008± 0.0012 for the shCHC until ~ 10 s, and 0.0121 ± 0.0018 for the shCHC after 10 s, exocytic rate: 0.0238 ± 0.0005 for the scrCHC, 0.0242 ± 0.0003 for the shCHC). CHC KD neurons also showed the slower kinetics of the post-stimulus endocytosis (Fig. 3 C; τ_{scrCHC}=15.58 ± 1.58 s, τ_{shCHC}=25.5 ± 2.01 s). These data indicated that blocking of CME by PITSTOP 2 treatment or CHC depletion, SVs membrane retrieval could be compensated by arising of CIE at low-frequency stimulation. In addition, post-stimulus endocytosis with CIE was slower than by occurring both CME and CIE.

Acute pharmacological inhibition of CIE did not contribute to SVs retrieval of the low-frequency stimulation

The next question was whether the endocytic defect and compensation during 5 Hz stimulation when CME was blocked could be also observed during the experimental condition in which CIE is blocked. To figure out this scenario, I treated BFA which is well known to inhibit transport from the endoplasmic reticulum to the Golgi complex indirectly by preventing the formation of coat protein 1 (COP1)-mediated transport vesicles [21] and is also known to block AP-1/-3-dependent SVs membrane retrieval via CIE [22]. Both DMSO treated and BFA treated neurons were stimulated with 200 APs, 5 Hz (Fig. 4 A1-2). Surprisingly, when CIE was blocked by BFA treatment, there was no defect of during- and post-stimulus endocytosis at 5 Hz stimulation (Fig. 4 B1-5 and C; endocytic rate: 0.009 ± 0.0007 for the control and 0.012 ± 0.0009 for the BFA treated, exocytic rate: 0.0239 ± 0.0001 for the control and 0.0244 ± 0.0002 for the BFA treated, and the time constant of after-stimulus endocytic kinetics: τ_{DMSO} = 11.35 ± 1.06 s, τ_{BFA} = 14.46 ± 1.32 s). I found that BFA-sensitive CIE pathway is dispensable at 5 Hz stimulation for SVs retrieval during and after stimulation.

The block of CIE by reducing endogenous AP-1/AP-3 also did not affect SVs retrieval during low-frequency stimulation

To test these remarkable results, I designed shRNAs using pSIREN vector which

targeted γ subunit of AP-1 and δ subunit of AP-3. AP-1 and AP-3 are known to be vital factor for SVs retrieval by CIE. In addition, deficiency of AP-1 not only affects the reformation of SVs from endosomes but also blocks the budding of bulk endosomes from the plasma membrane [22]. Then, I conducted exo/endocytosis assay again with AP-1 KD, and AP-3 KD neurons at 5 Hz stimulation, subsequently (Fig. 5 A1-2 and Fig. 6 A1-2). The endocytic and exocytic kinetics of AP-1 depleted neurons were similar with the kinetics of control neurons during 5 Hz stimulation (Fig. 5 B1-3). Their post–stimulation kinetics and time constant values were also similar with those of the control group (Fig. 5 C; $\tau_{scrAP\text{-}1} = 16.00 \pm 1.02$ s, and $\tau_{shAP\text{-}1} = 14.32 \pm 2.17$ s).

Moreover, AP-3 has also been implicated in SVs recycling [22, 23] and the lack of AP-3 is able to defect in SVs recycling and biogenesis [24]. Kinetics of AP-3 downregulated neurons was nearly identical with that of the control neurons (Fig. 6 B1-3). Whether AP-3 depleted or not, neurons has insignificant impact on the rate of SVs retrieval as well as after-stimulus endocytosis (Fig. 6 C; $\tau_{scrAP\text{-}3} = 16.55 \pm 1.68$ s, and $\tau_{shAP\text{-}3} = 15.73 \pm 0.67$ s). The knockdown of AP-1 and AP-3, like BFA, did not show any particular defect of endocytosis at 5 Hz stimulation. As before I have found, CIE pathway is dispensable in a moderate frequency stimulation for SVs retrieval during- and after- stimulation. Considering all these 5 Hz stimulation data, CME is the major pathway of SVs retrieval at the low-frequency stimulation. Thus, when CME is blocked, CIE make up for the endocytic deficiency, but CIE could not completely retrieve SVs at during-and post-stimulation.

The mode of CME is gratuitous for plasma membrane retrieval under conditions of high-frequency stimulation

How SVs membranes are retrieved during high-frequency stimulation, and which pathway operate dominantly? To ascertain rational answers to this questions, I performed exo/endocytosis assay at 40 Hz, 200 APs with blockage of each endocytosis pathway. In the first place, to determine whether CME is still prominent or not, CME was blocked with PITSTOP 2 treatment because its predominance under conditions of low-frequency. Pre-incubated neurons with DMSO or PITSTOP 2 were electrically stimulated at 40 Hz frequency with or without *Foli* (Fig. 7 A1-2). Interestingly, exo/endocytosis proceeded unaltered in CME inhibited neurons with a near-identical τ value to that measured in control neurons (Fig. 7 C; $\tau_{DMSO} = 13.25 \pm 1.14$ s, and $\tau_{PITSTOP\ 2} = 15.93 \pm 1.73$ s). When high-frequency stimulation was performed, after early phase delay, few amount of during-stimulus endocytosis were occurred in control neurons. Likewise, when CME was blocked by application of PITSTOP 2, during-stimulus endocytosis was not further impeded than the control (Fig. 7 B1-5; endocytic rate: 0.0054 ± 0.0198 (early phase), 0.0439 ± 0.0197 (after delay) for the control, and 0.0107 ± 0.0064 (early phase), 0.0307 ± 0.0098 (after delay) for the PITSTOP 2). At low-frequency stimulation, CME of PITSTOP 2 treated neurons were blocked at early phase of during-stimulus endocytosis and not retrieved completely after stimulation at the low-frequency. However, both during- and post-high frequency stimulus endocytosis were unaffected by blockage of CME. This data implied that CME is minor pathway at 40

Hz stimulation and CIE is superior in this conditions.

To confirm these observations, I performed the same process at CHC knockdown synapses (Fig. 8). Reducing CME by clathrin knockdown hardly affected membrane retrieval during- and after-stimulus in 40 Hz (Fig. 8 B1-5 and C; endocytic rate: 0.0077 ± 0.0170 for the scrCHC until ~2 s, 0.0478 ± 0.0107 for the scrCHC after 2 s, 0.0006 ± 0.0062 for the shCHC until ~ 2 s, and 0.0396 ± 0.0093 for the shCHC after 2 s, exocytic rate: 0.1678 ± 0.0025 for the scrCHC and 0.1687 ± 0.0013 for the shCHC, τ_{scrCHC}=13.15 ± 2.36 s, τ_{shCHC} =16.38 ± 1.74 s). In total, blockage of CME by both downregulating endogenous clathrin level and using PITSTOP 2 did not disrupt during- and post-stimulus endocytosis at intense frequency stimulation.

The frequency of stimulation modulates the pathway of SVs retrieval toward effective way

To assess the contribution of CIE mode at high-frequency stimulation, I used BFA to block the CIE and discovered that there was a tremendous effect. After the 40 Hz stimulation without *Foli*, the fluorescence of vGpH failed to recover to its initial value. This phenomenon suggests that retrieval of the released SVs was incompletely and about 40 % of vGpH remained at the plasma membrane. (Fig. 9 A2). Compared to the control neurons, the kinetics and rate constant of after-stimulus endocytosis in BFA treated neurons were approximately three times slower (Fig. 9 A1-2 and C). Intriguingly,

in measuring the rate of pure exocytosis after the second stimulation with *Foli*, the fluorescence of vGpH only increased to the peak value of the first stimulation. This indicates that in the presence of BFA, the exocytic SVs after the second stimulation were the SVs that were retrieved from the first stimulation via the BFA-insensitive retrieval pathway. From this result, I extended the linear curve representing the normalized fluorescence from 0 to 1 with the slope value remaining unchanged for the second stimulation in the presence of *foli*. Then, to measure the speed of during-stimulus endocytosis, I subtracted the fluorescence of vGpH in the first stimulation from the normalized data during the second stimulation. Based on this method, the presence of BFA completely abolished the endocytosis during high-frequency stimulation (Fig. 9 B1-5). Considering all the 40 Hz data, I confirmed that CIE is the major pathway at high-frequency stimulation. While the CIE blockage completely abolished the endocytosis during stimulation, CME inhibition did not affect the process. After-stimulus endocytosis was also not affected by CME inhibition although the CIE blockage slowed the process. The experimental findings showed that mature hippocampal neurons have evolved mechanisms of modulation between CIE and CME to ensure the efficient membrane retrieval based on the stimulation frequencies. In addition, when either one pathway is blocked, the other pathway can compensate for the deficiency.

Figure 1.

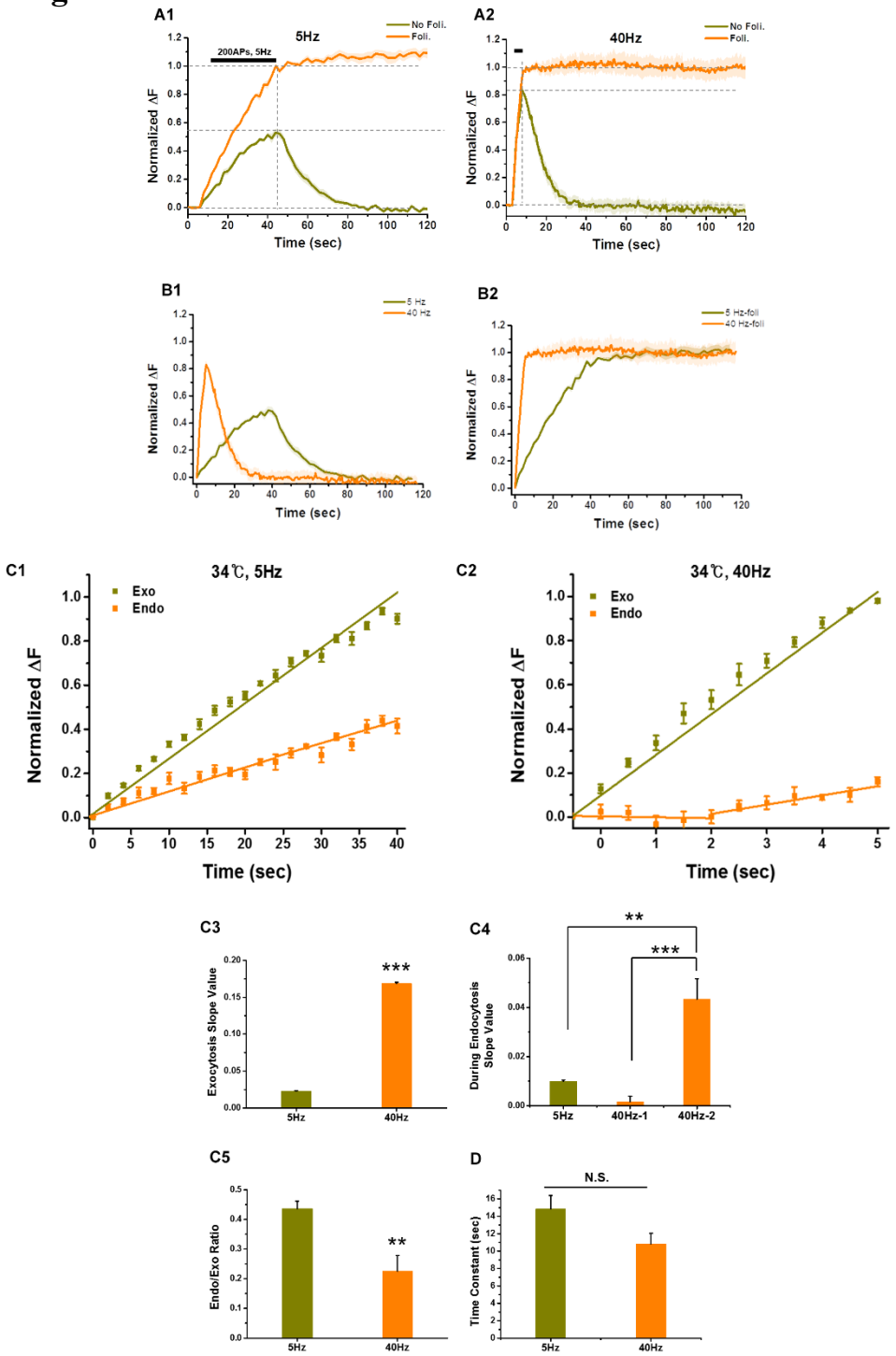
A1
5Hz
No Foli.
Foli.
200APs, 5Hz
Normalized ΔF
Time (sec)
A2
40Hz
No Foli.
Foli.
Normalized ΔF
Time (sec)
B1
5 Hz
40 Hz
Normalized ΔF
Time (sec)
B2
5 Hz-foli
40 Hz-foli
Normalized ΔF
Time (sec)
C1
34℃, 5Hz
Exo
Endo
Normalized ΔF
Time (sec)
C2
34℃, 40Hz
Exo
Endo
Normalized ΔF
Time (sec)
C3
Exocytosis Slope Value
***
5Hz
40Hz
C4
**
***
During Endocytosis Slope Value
5Hz
40Hz-1
40Hz-2
C5
Endo/Exo Ratio
**
5Hz
40Hz
D
N.S.
Time Constant (sec)
5Hz
40Hz

Figure 1. SVs membrane retrieval is modulated by stimulation frequency in hippocampal neurons.

A1-A2, Average traces of hippocampal neurons expressing vGpH in response to 200 APs applied at 5 Hz or 40 Hz in DIV 16. The fluorescence intensity profiles from 5 Hz **(A1)** and 40 Hz **(A2)** synapses stimulated without Folimycin (*Foli*), at first. After a 7 min for resting, the same neurons were stimulated again with an identical stimulation in the presence of *Foli*. In the absence of the *Foli*, the fluorescence signal reflects the net balance of exocytosis and endocytosis. In the presence of the *Foli*, exocytosis events were trapped in an alkaline state, and the fluorescence signal reflected exocytosis (ΔF_{Exo}). Fluorescence values were normalized to the maximal fluorescence change after 200 APs in the *Foli* trace ($n = 262$ neurons from 9 independent coverslips for the 5 Hz and $n = 97$ neurons from 5 independent coverslips for the 40 Hz). Error bars indicate SEM.

B1-B2, Compare to the peak and average traces of fluorescence between two frequencies, the fluorescence intensity merged based on the imaging time. Representative averaged vGpH traces in response to 200 APs at 5 Hz or 40 Hz in the absence **(B1)** or presence of *Foli* **(B2)**.

C1-C2, Graphs showing the time course of endocytosis (Endo) and exocytosis (Exo) during the stimulation with 200 APs at each frequencies (**C1**: 5 Hz and **C2**: 40 Hz). Time course of endocytosis during stimulation was derived by subtracting the fluorescence in the absence of the *Foli* ($\Delta F_{exo-endo}$) from the fluorescence in its presence ($\Delta F_{endo} = \Delta F_{exo} - \Delta F_{exo-endo}$). Rate of exocytosis and rate of endocytosis during-stimulus

were obtained from the linear fits to whole time during stimulation. **C3-C4,** Bar graph showed the average slope of exocytosis and endocytosis. In the 40 Hz, the linear fits were done separately based on 2 s, because of the fluorescence intensity profiled the brief delay until ~2 s. (exocytic rate: 0.0226 ± 0.0004 for the 5 Hz, 0.1683 ± 0.0019 for the 40 Hz; endocytic rate: 0.0099 ± 0.0006 for the 5 Hz, 0.0034 ± 0.0115 for the 40 Hz until ~ 2 s, and 0.0433 ± 0.0082 for the 40 Hz after 2 s). **C5,** Ratios of endocytosis/exocytosis rate resulted 0.4468 ± 0.0252 for the 5 Hz, 0.2255 ± 0.0525 for the 40 Hz. Data are presented as means ± SE. **p < 0.01 and ***p < 0.001(Student's *t*-test, ANOVA and LSD post hoc test)

D, Decay of post-stimulus fluorescence of vGpH fitted by double exponential with time constant, τ = 15.79 ± 1.38 s for the 5 Hz and 11.82 ± 1.20 s for the 40 Hz.

Figure 2.

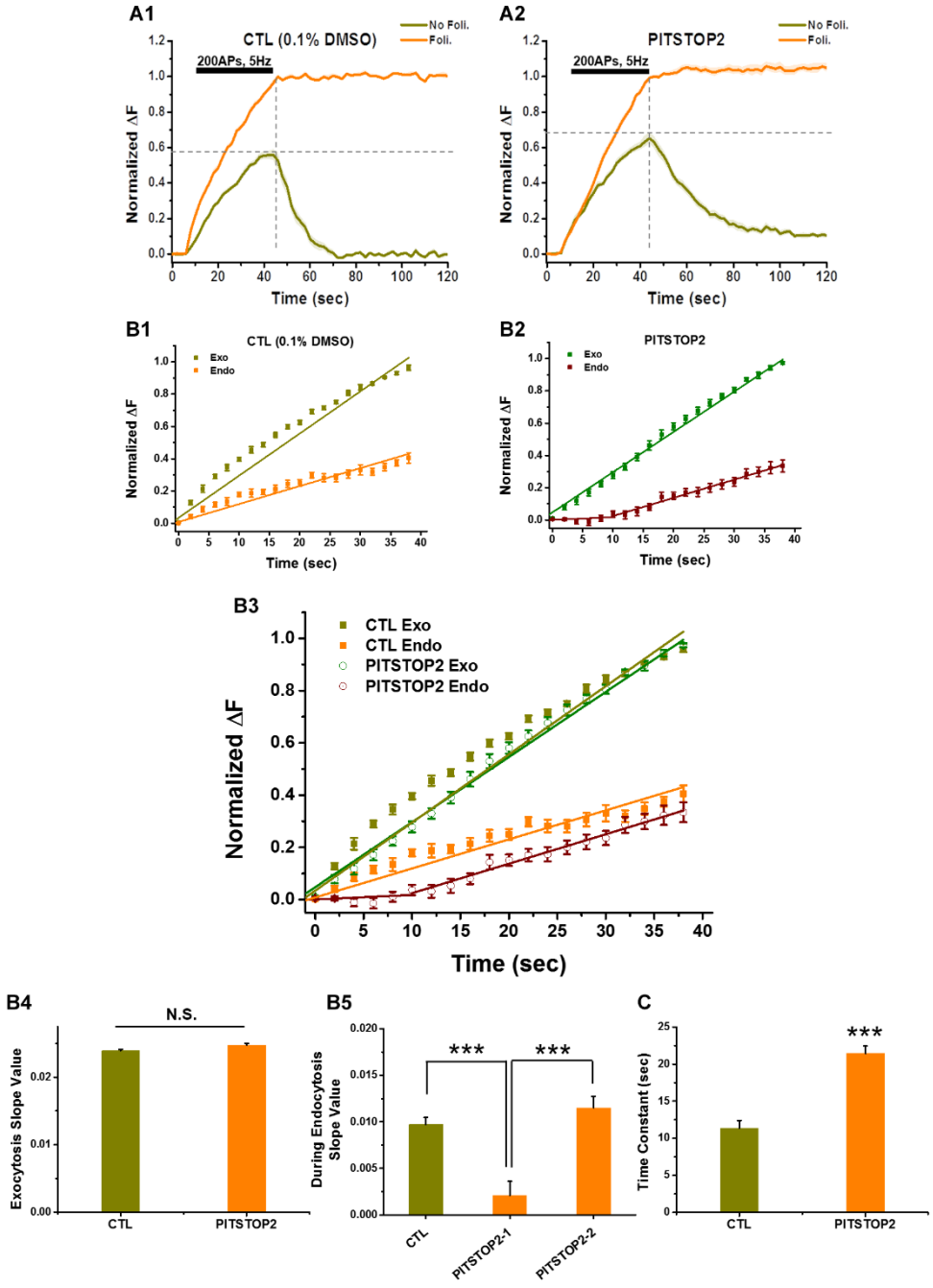
A1
CTL (0.1% DMSO)
No Foli.
Foli.
200APs, 5Hz
Normalized ΔF
Time (sec)
A2
PITSTOP2
No Foli.
Foli.
200APs, 5Hz
Normalized ΔF
Time (sec)
B1
CTL (0.1% DMSO)
Exo
Endo
Normalized ΔF
Time (sec)
B2
PITSTOP2
Exo
Endo
Normalized ΔF
Time (sec)
B3
CTL Exo
CTL Endo
PITSTOP2 Exo
PITSTOP2 Endo
Normalized ΔF
Time (sec)
B4
N.S.
Exocytosis Slope Value
CTL
PITSTOP2
B5
***
***
During Endocytosis Slope Value
CTL
PITSTOP2-1
PITSTOP2-2
C
***
Time Constant (sec)
CTL
PITSTOP2

Figure 2. Blockage of CME by using PITSTOP 2 lead to during- and post-stimulus endocytic defect at low-frequency stimulation.

A1-A2, Average traces of vGpH fluorescence intensity profiles neurons from **(A1)** the control (0.1 % DMSO) and **(A2)** 30 min treatment of 25 μM PITSOP2 stimulated with or without *Foli*. Neurons were stimulated at 5 Hz, 200 APs with two consecutive stimuli with 7 min break between the stimuli. Fluorescence values were normalized to the maximal fluorescence change after 200 APs in the *Foli* trace (n = 110 neurons from 6 independent coverslips for the control and n = 155 neurons from 7 independent coverslips for the PITSTOP 2 treatment). Membrane retrieval induced by low-frequency stimulation is significantly slowed in the block of CME by PITSTOP 2. Error bars indicate SEM.

B1-B3, Graphs showing the time course of endocytosis (Endo) and exocytosis (Exo) during stimulation with 200 APs at 5 Hz. Rate of exocytosis and rate of endocytosis during-stimulus were obtained from the linear fits to the whole time during stimulation. During-stimulus endocytosis of the PITSTOP 2 treated neurons **(B2)** was halted until ~ 10 s, while the Control **(B1)** retrieved SVs well during the stimulation. **(B3)** Those data were merged and displayed based on the time of imaging. In case of PITSTOP 2 treatment, because of the fluorescence intensity showed that during-stimulus was stopped until ~10 s, the data fitted by a linear apart based on 10 s. **B4-B5,** Bar graph showed the average slope of exocytosis **(B4)** and endocytosis **(B5)** (exocytic rate: 0.0239 ± 0.0001 for the control, 0.0243 ± 0.0003 for the PITSTOP 2 treated; endocytic

rate: 0.009 ± 0.0007 for the control, 0.002 ± 0.0010 for the PITSTOP 2 treated until ~ 10 s, and 0.0115 ± 0.0013 for the PITSTOP 2 treated after 10 s). Data are presented as means ± SE. ***p < 0.001(Student's *t*-test, ANOVA and LSD post hoc test)

C, Decay of post-stimulus fluorescence of vGpH fitted by double exponential with time constant, $\tau = 11.35 \pm 1.06$ s for the control and 21.45 ± 0.98 s for the PITSTOP 2 treated neurons. Data are presented as means ± SE. ***p<0.001 (Student's *t*-test).

Figure 3.

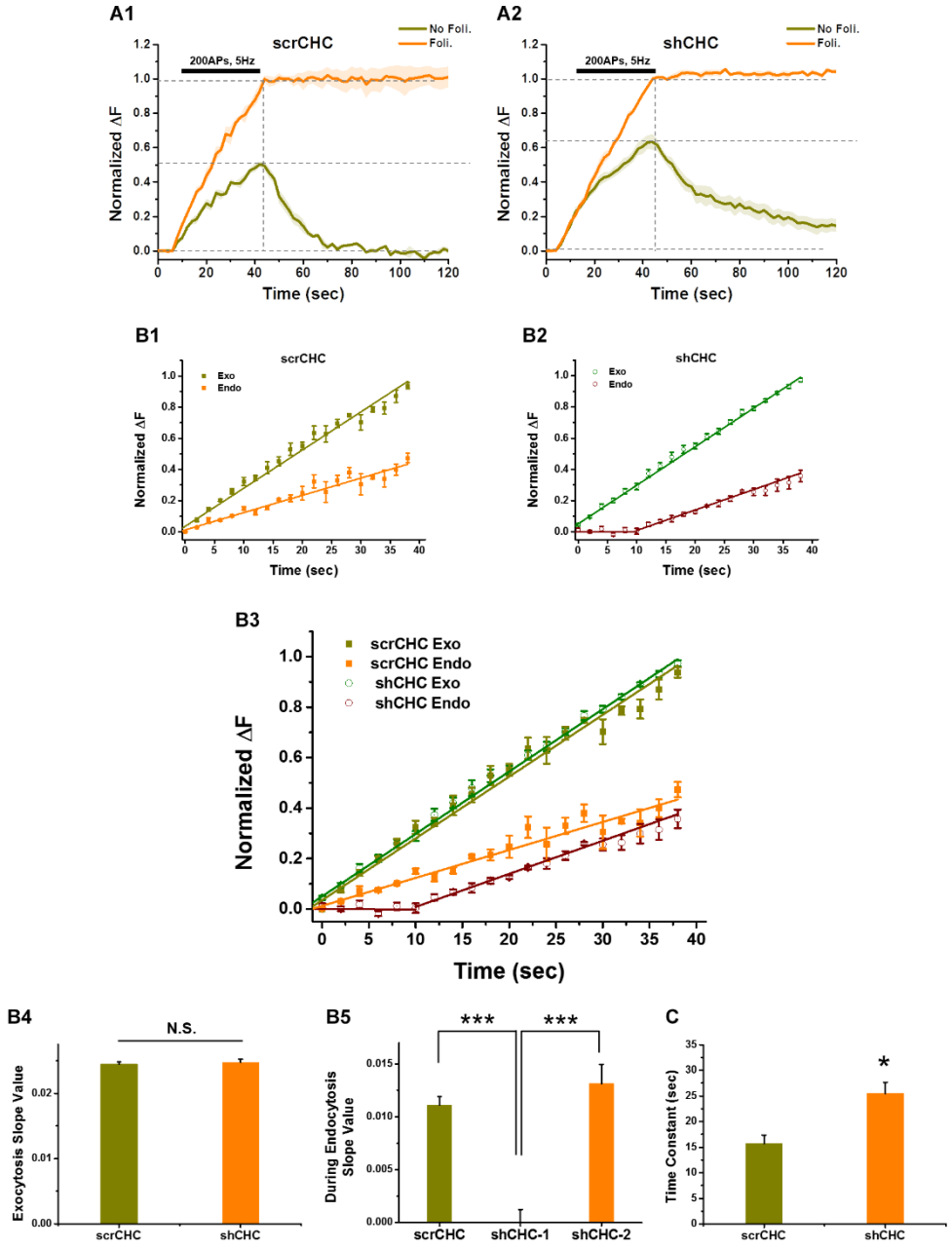
A1
scrCHC
No Foli.
Foli.
200APs, 5Hz
Normalized ΔF
Time (sec)
A2
shCHC
No Foli.
Foli.
200APs, 5Hz
Normalized ΔF
Time (sec)
B1
scrCHC
Exo
Endo
Normalized ΔF
Time (sec)
B2
shCHC
Exo
Endo
Normalized ΔF
Time (sec)
B3
scrCHC Exo
scrCHC Endo
shCHC Exo
shCHC Endo
Normalized ΔF
Time (sec)
B4
N.S.
Exocytosis Slope Value
scrCHC
shCHC
B5
***
***
During Endocytosis Slope Value
scrCHC
shCHC-1
shCHC-2
C
*
Time Constant (sec)
scrCHC
shCHC

Figure 3. Deletion of endogenous clathrin by shRNA also lead to during- and post-stimulus endocytic defect at low-frequency stimulation.

A1-A2, Hippocampal neurons were transfected with shRNA targeted for CHC or respective scrambled shRNA. Average vGpH fluorescence intensity profiles of the boutons from the scrambled CHC **(A1)** or the shRNA CHC **(A2)** with 200 APs at 5 Hz stimulation at DIV 16 with absence or presence of *Foli*. (n = 81 neurons from 4 independent coverslips for the scrCHC and n = 92 neurons from 5 independent coverslips for the shCHC) Error bars indicate SEM.

B1-B3, Graphs showing the time course of endocytosis (Endo) and exocytosis (Exo) during stimulation with 200 APs at 5 Hz. Rate of exocytosis and rate of endocytosis during-stimulus were obtained from the linear fits to whole time during the stimulation. During-stimulus endocytosis of the shCHC neurons **(B2)** was halted few seconds, while the scrCHC **(B1)** retrieved SVs well during stimulation. **(B3)** Those data were merged and displayed based on the time of imaging. At the shCHC, the data fitted by a linear apart based on 10 s. **B4-B5,** Bar graph showed the average slope of exocytosis **(B4)** and endocytosis **(B5)** (exocytic rate: 0.0238 ± 0.0005 for the scrCHC, 0.0242 ± 0.0003 for the shCHC; endocytic rate: 0.0113 ± 0.0007 for the scrCHC, 0.0008± 0.0012 for the shCHC until ~ 10 s, and 0.0121 ± 0.0018 for the shCHC after 10 s). Data are presented as means ± SE. ***p < 0.001(Student's *t*-test, ANOVA and LSD post hoc test)

C, The decay of vGpH was fitted by double exponential with time constant, $\tau = 15.58 \pm 1.58$ s for the scrCHC and $\tau = 25.5 \pm 2.01$ s for the shCHC, respectively. Data are presented as means ± SE (Student's *t*-test).

Figure 4.

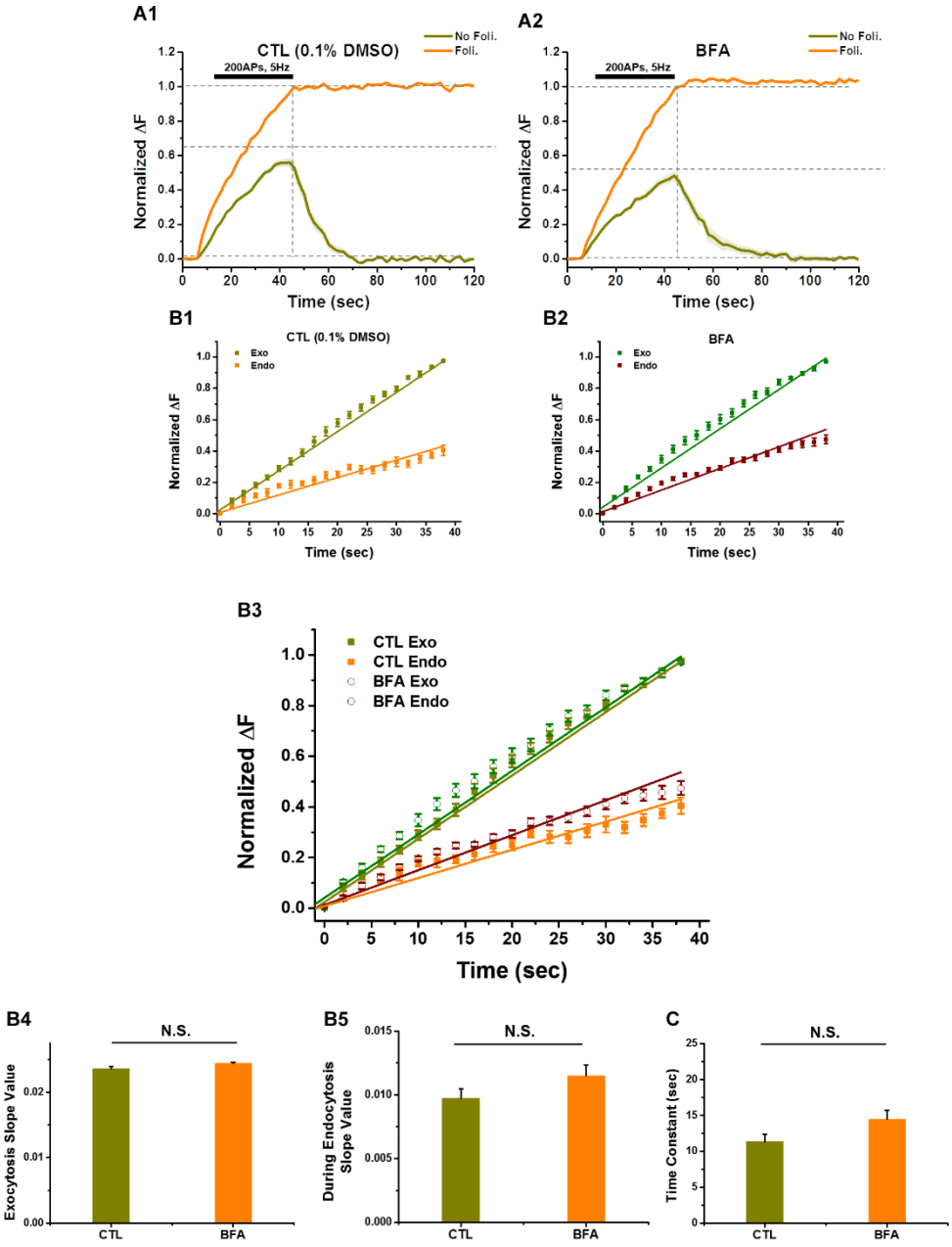
A1
CTL (0.1% DMSO)
No Foli.
Foli.
200APs, 5Hz
Normalized ΔF
Time (sec)
A2
BFA
No Foli.
Foli.
200APs, 5Hz
Normalized ΔF
Time (sec)
B1
CTL (0.1% DMSO)
Exo
Endo
Normalized ΔF
Time (sec)
B2
BFA
Exo
Endo
Normalized ΔF
Time (sec)
B3
CTL Exo
CTL Endo
BFA Exo
BFA Endo
Normalized ΔF
Time (sec)
B4
N.S.
Exocytosis Slope Value
CTL
BFA
B5
N.S.
During Endocytosis Slope Value
CTL
BFA
C
N.S.
Time Constant (sec)
CTL
BFA

Figure 4. Acute pharmacological inhibition of CIE was not contributed to SVs retrieval of the low-frequency stimulation.

A1-A2, Average vGpH fluorescence intensity profiles of the boutons from after 30 min treatment of 0.1 % DMSO, as a control, **(A1)** or after of 10 μg/ml BFA **(A2)** with 200 APs at 5 Hz stimulation with or without *Foli*. Note that regardless of CIE blockage, the SVs retrieval is unaffected during- and post- stimulation. (n = 110 neurons from 6 independent coverslips for the control and n = 142 neurons from 6 independent coverslips for the BFA treatment). Error bars indicate SEM.

B1-B3, Graphs showed the time course of endocytosis (Endo) and exocytosis (Exo) during stimulation with 200 APs at 5 Hz. Rate of exocytosis and rate of endocytosis during-stimulus were obtained from the linear fits to whole time during stimulation. During-stimulus endocytic slope of the control **(B1)** and the BFA treated neurons **(B2)** were approximately equal. **(B3)** Those data were merged and displayed based on the time of imaging. **B4-B5,** Bar graph showed the average slope value of exocytosis **(B4)** and endocytosis **(B5)**. (exocytic rate: 0.0239 ± 0.0001 for the control and 0.0244 ± 0.0002 for the BFA treated; endocytic rate: 0.009 ± 0.0007 for the control and 0.012 ± 0.0009 for the BFA treated). Data are presented as means ± SE. (Student's *t*-test)

C, Decay of post-stimulus fluorescence of vGpH fitted by double exponential with time constant, τ = 11.35 ± 1.06 s for the control and 14.46 ± 1.32 s for the BFA treatment. Data are presented as means ± SE (Student's *t*-test).

Figure 5.

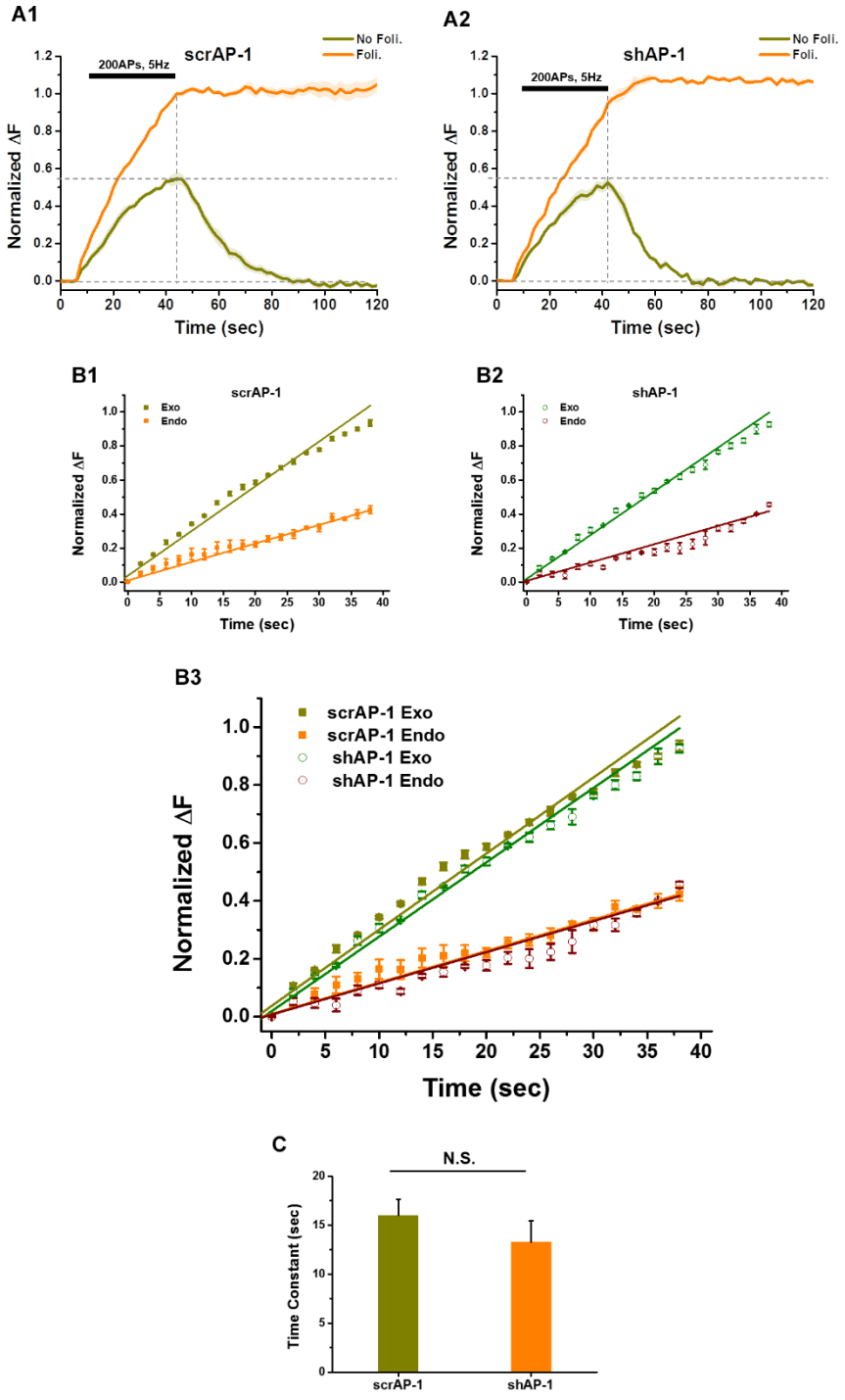
A1
scrAP-1
200APs, 5Hz
No Foli.
Foli.
Normalized ΔF
Time (sec)
A2
shAP-1
200APs, 5Hz
No Foli.
Foli.
Normalized ΔF
Time (sec)
B1
scrAP-1
Exo
Endo
Normalized ΔF
Time (sec)
B2
shAP-1
Exo
Endo
Normalized ΔF
Time (sec)
B3
scrAP-1 Exo
scrAP-1 Endo
shAP-1 Exo
shAP-1 Endo
Normalized ΔF
Time (sec)
C
N.S.
Time Constant (sec)
scrAP-1
shAP-1

Figure 5. The block of CIE by reducing endogenous AP-1 also did not affect SVs retrieval during low-frequency stimulation.

A1-A2, Average vGpH fluorescence intensity profiles of the boutons from transfected shRNA of AP-1 **(A2)** and respectively scrambled **(A1)** with 200 APs at 5 Hz stimulation with or without *Foli*. Blockage of CIE by using shRNA to inhibit AP-1 protein also resulted in no defect in the SVs retrieval. (n = 79 neurons from 5 independent coverslips for the scrAP-1 and n = 91 neurons from 4 independent coverslips for the shAP-1). Error bars indicate SEM.

B1-B3, Graphs showed the time course of endocytosis (Endo) and exocytosis (Exo) during stimulation with 200 APs at 5 Hz. Rate of exocytosis and rate of endocytosis during-stimulus were obtained from the linear fits to whole time during stimulation. During-stimulus endocytic slope of the scrAP-1 **(B1)** was almost identical with the shAP-1 neurons **(B2)**. **(B3)** Those data were merged and displayed based on the time of imaging. Error bars indicate SEM.

C, Decay of post-stimulus fluorescence of vGpH fitted by double exponential with time constant, $\tau = 16.00 \pm 1.02$ s for the scrAP-1 and 14.32 ± 2.17 s for the shAP-1. Data are presented as means ± SE (Student's *t*-test).

Figure 6.

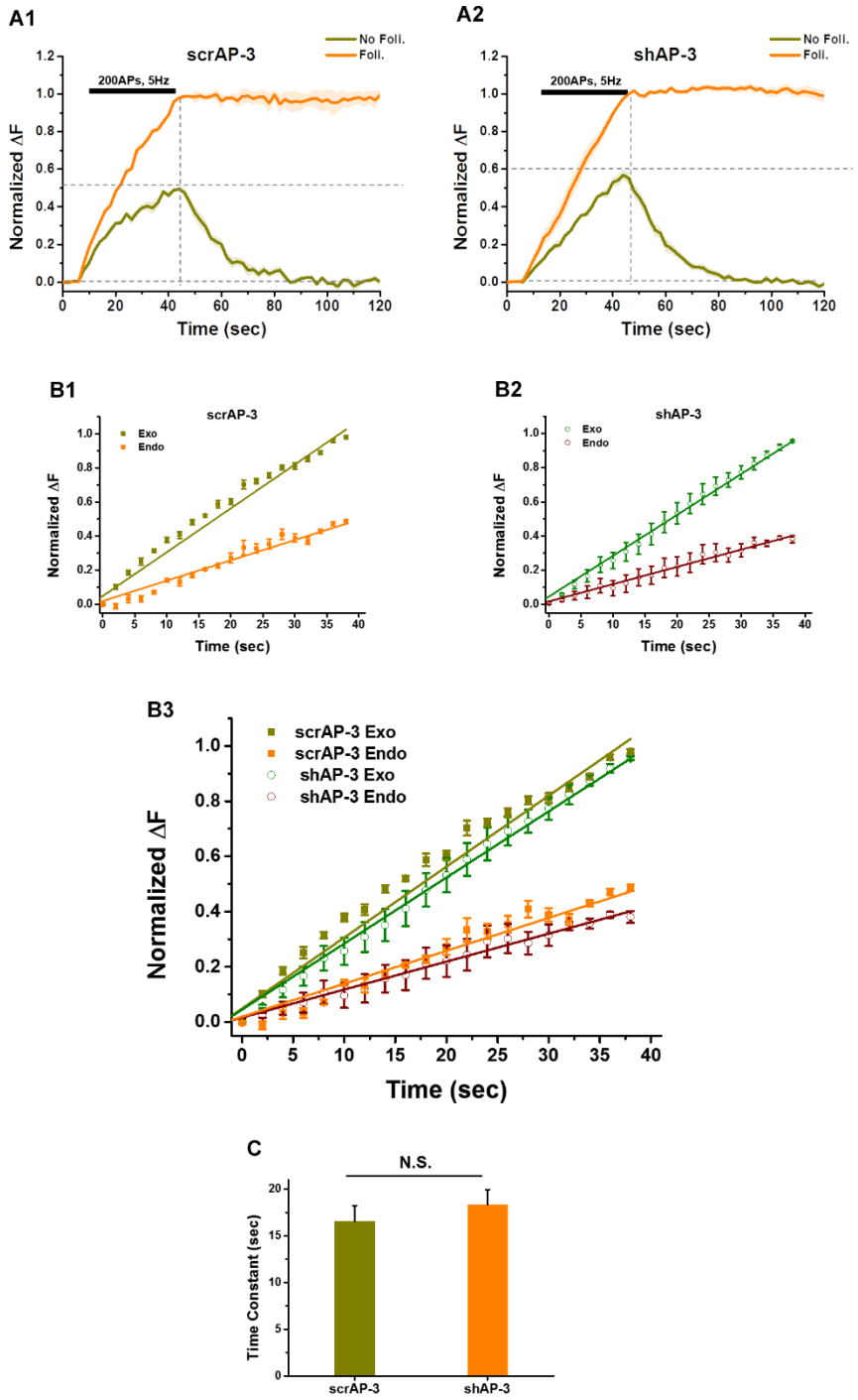
A1
scrAP-3
No Foll.
Foll.
200APs, 5Hz
Normalized ΔF
Time (sec)
A2
shAP-3
No Foll.
Foll.
200APs, 5Hz
Normalized ΔF
Time (sec)
B1
scrAP-3
Exo
Endo
Normalized ΔF
Time (sec)
B2
shAP-3
Exo
Endo
Normalized ΔF
Time (sec)
B3
scrAP-3 Exo
scrAP-3 Endo
shAP-3 Exo
shAP-3 Endo
Normalized ΔF
Time (sec)
C
N.S.
Time Constant (sec)
scrAP-3
shAP-3

Figure 6. Reduction of AP-3 by shRNA did not contribute to SVs retrieval at low-frequency stimulation.

A1-A2, Hippocampal neurons were expressed the shRNA target of AP-3 and scrambled respectively. Average vGpH fluorescence intensity profiles of the boutons from expressed shRNA of AP-3 **(A2)** and scrambled AP-3**(A1)** with 200 APs at 5 Hz stimulation with or without *Foli*. Depletion of AP-3 by shRNA was also largely unaffected to endocytosis during low-frequency stimulation. (n = 81 neurons from 4 independent coverslips for the scrAP-3 and n = 106 neurons from 4 independent coverslips for the shAP-3). Error bars indicate SEM.

B1-B3, Slope of the graphs showing the time course of endocytosis (Endo) and exocytosis (Exo) during stimulation with 200 APs at 5 Hz. Rate of exocytosis and rate of endocytosis during-stimulus were obtained from the linear fits to whole time during stimulation. During-stimulus endocytic slope of the scrAP-3 **(B1)** was almost identical with the shAP-3 neurons **(B2)**. **(B3)** Those data were merged and displayed based on the time of imaging. Error bars indicate SEM.

C, The decay of vGpH was fitted by double exponential with time constant, $\tau = 16.55 \pm 1.68$ s for the scrAP-3 and $\tau = 15.73 \pm 0.67$ s for the shAP-3, respectively. Data are presented as means ± SE (Student's *t*-test).

Figure 7.

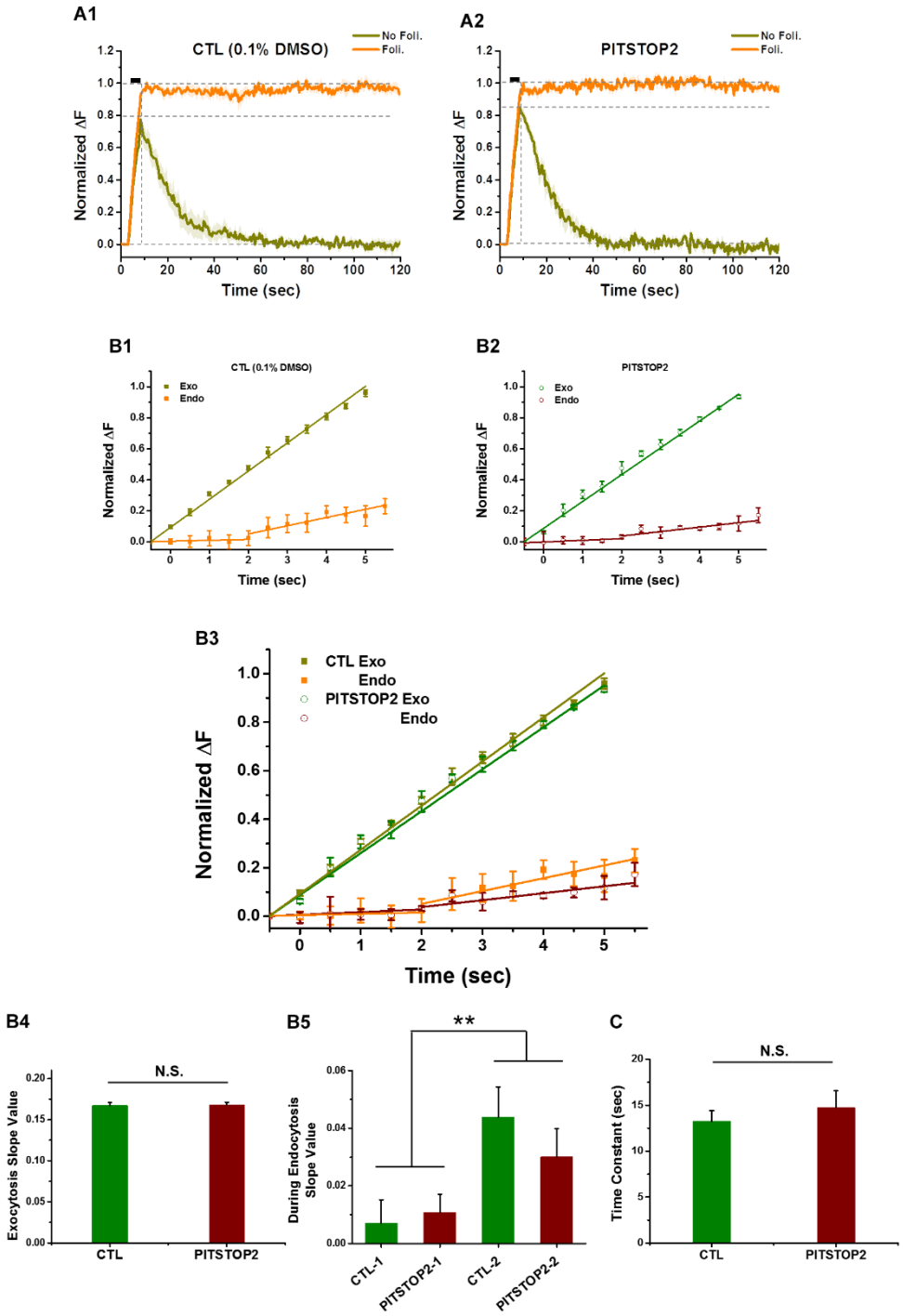
A1
CTL (0.1% DMSO)
No Foli.
Foli.
Normalized ΔF
Time (sec)
A2
PITSTOP2
B1
CTL (0.1% DMSO)
Exo
Endo
B2
PITSTOP2
B3
CTL Exo
Endo
PITSTOP2 Exo
Endo
B4
N.S.
Exocytosis Slope Value
CTL
PITSTOP2
B5
**
During Endocytosis Slope Value
CTL-1
PITSTOP2-1
CTL-2
PITSTOP2-2
C
N.S.
Time Constant (sec)
CTL
PITSTOP2

Figure 7. Defect of endocytosis and reacidification were not detected in CME blocked neurons by using PITSTOP 2 at high-frequency stimulation.

A1-A2, Neurons were treated and 30 min incubated with 0.1 % DMSO as a control **(A1)**, and 25 μM PITSTOP 2 **(A2)**. Average vGpH fluorescence intensity profiles of the neurons stimulated with 200 APs at 40 Hz in the presence or absence of *Foli*. (*n* = 122 neurons from 4 independent coverslips for the control and *n* = 83 neurons from 5 independent coverslips for the PITSTOP 2 treated) Data are presented as means ± SEM. **B1-B3,** The graphs give the rates of endocytosis (Endo) and exocytosis (Exo) during stimulation with 200 APs at 40 Hz. The traces obtained in the presence and in the absence of *Foli* were normalized to the maximum fluorescence signal the end of stimulation after *Foli* treatment. Rate of exocytosis and rate of endocytosis during-stimulus were obtained from the linear fits to the data during stimulation. In case of the high-frequency stimulation, the data fitted separately at two second due to the fact that the during-stimulus endocytosis is expelled until ~ 2 s. During-stimulus endocytic slope of the control **(B1)** and PITSTOP 2 treated neurons **(B2)** were approximately equal. **(B3)** Those data were merged and displayed based on the time of imaging. **B4-B5,** Bar graph showed the average slope value of exocytosis **(B4)** and endocytosis **(B5)**. (exocytic rate: 0.1672 ± 0.0035 for the control and 0.1679 ± 0.0033 for the PITSTOP 2; endocytic rate: 0.0054 ± 0.0198 for the control until ~2 s, 0.0439 ± 0.0197 for the control after 2 s, 0.0107 ± 0.0064 for the PITSTOP 2 treated until ~ 2 s, and 0.0307 ± 0.0098 for the

PITSTOP 2 treated after 2 s). Data are presented as means ± SE. **p < 0.01(Student's *t*-test and ANOVA with LSD post hoc test)

C, Decay of post-stimulus fluorescence of vGpH fitted by double exponential with time constant, τ = 13.25 ± 1.14 s for the control and 15.93 ± 1.73 s for the PITSTOP 2 treated. Data are presented as means ± SE (Student's *t*-test).

Figure 8.

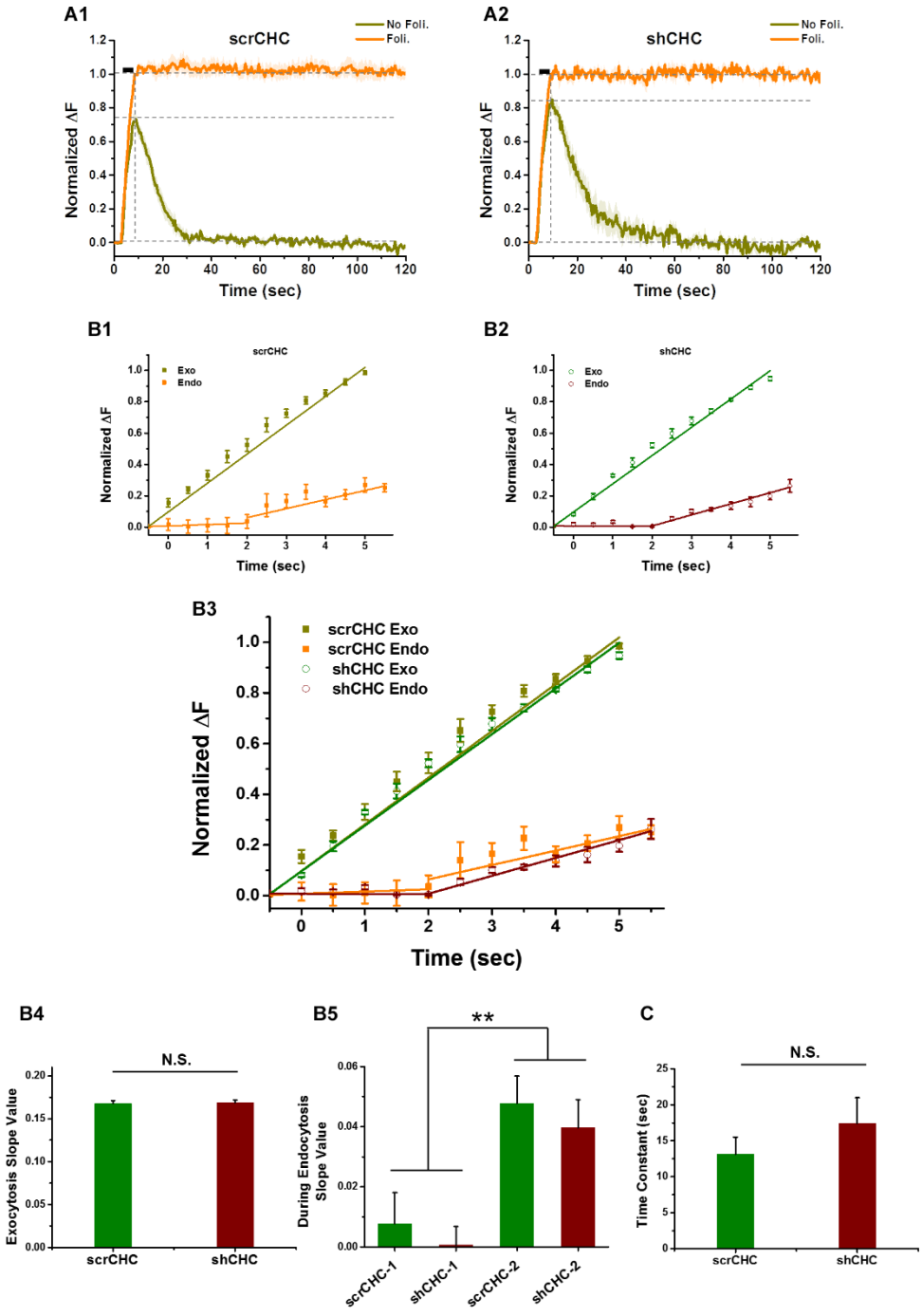
A1
scrCHC
No Foli.
Foli.
Normalized ΔF
Time (sec)
A2
shCHC
No Foli.
Foli.
Normalized ΔF
Time (sec)
B1
scrCHC
Exo
Endo
Normalized ΔF
Time (sec)
B2
shCHC
Exo
Endo
Normalized ΔF
Time (sec)
B3
scrCHC Exo
scrCHC Endo
shCHC Exo
shCHC Endo
Normalized ΔF
Time (sec)
B4
N.S.
Exocytosis Slope Value
scrCHC
shCHC
B5
**
During Endocytosis Slope Value
scrCHC-1
shCHC-1
scrCHC-2
shCHC-2
C
N.S.
Time Constant (sec)
scrCHC
shCHC

Figure 8. Depletion of clathrin was also not affected SVs retrieval at high-frequency stimulation.

A1-A2, Hippocampal neurons were transfected with shRNA targeted for CHC or respective scrambled shRNA. Average vGpH fluorescence intensity profiles of the neurons from the scrambled CHC **(A1)** or the shRNA CHC **(A2)** with 200 APs at 40 Hz stimulation at DIV 16 with absence or presence of *Foli*. (n = 72 neurons from 5 independent coverslips for the scrCHC and n = 63 neurons from 4 independent coverslips for the shCHC) Error bars indicate SEM.

B1-B3, Graphs showing the time course of endocytosis (Endo) and exocytosis (Exo) during stimulation with 200 APs at 40 Hz. Rate of exocytosis and rate of endocytosis during-stimulus were obtained from the linear fits to the whole time during stimulation. Because of the during-stimulus endocytosis is expelled until ~ 2 s at high-frequency stimulation, the data fitted separately at two second. During-stimulus endocytic slope of the scrCHC **(B1)** and the shCHC transfected neurons **(B2)** were approximately equal. **(B3)** Those data were merged and displayed based on the time of imaging. **B4-B5,** Bar graph showed the average slope value of exocytosis **(B4)** and endocytosis **(B5)** (exocytic rate: 0.1678 ± 0.0025 for the scrCHC and 0.1687 ± 0.0013 for the shCHC; endocytic rate: 0.0077 ± 0.0170 for the scrCHC until ~2 s, 0.0478 ± 0.0107 for the scrCHC after 2 s, 0.0006 ± 0.0062 for the shCHC until ~ 2 s, and 0.0396 ± 0.0093 for the shCHC after 2 s). Data are presented as means ± SE. **p < 0.01(Student's *t*-test and ANOVA with LSD post hoc test)

C, The decay of vGpH was fitted by double exponential with time constant, $\tau = 13.15 \pm 2.36$ s for the scrCHC and $\tau = 16.38 \pm 1.74$ s for the shCHC, respectively. Data are presented as means ± SE (Student's *t*-test).

Figure 9.

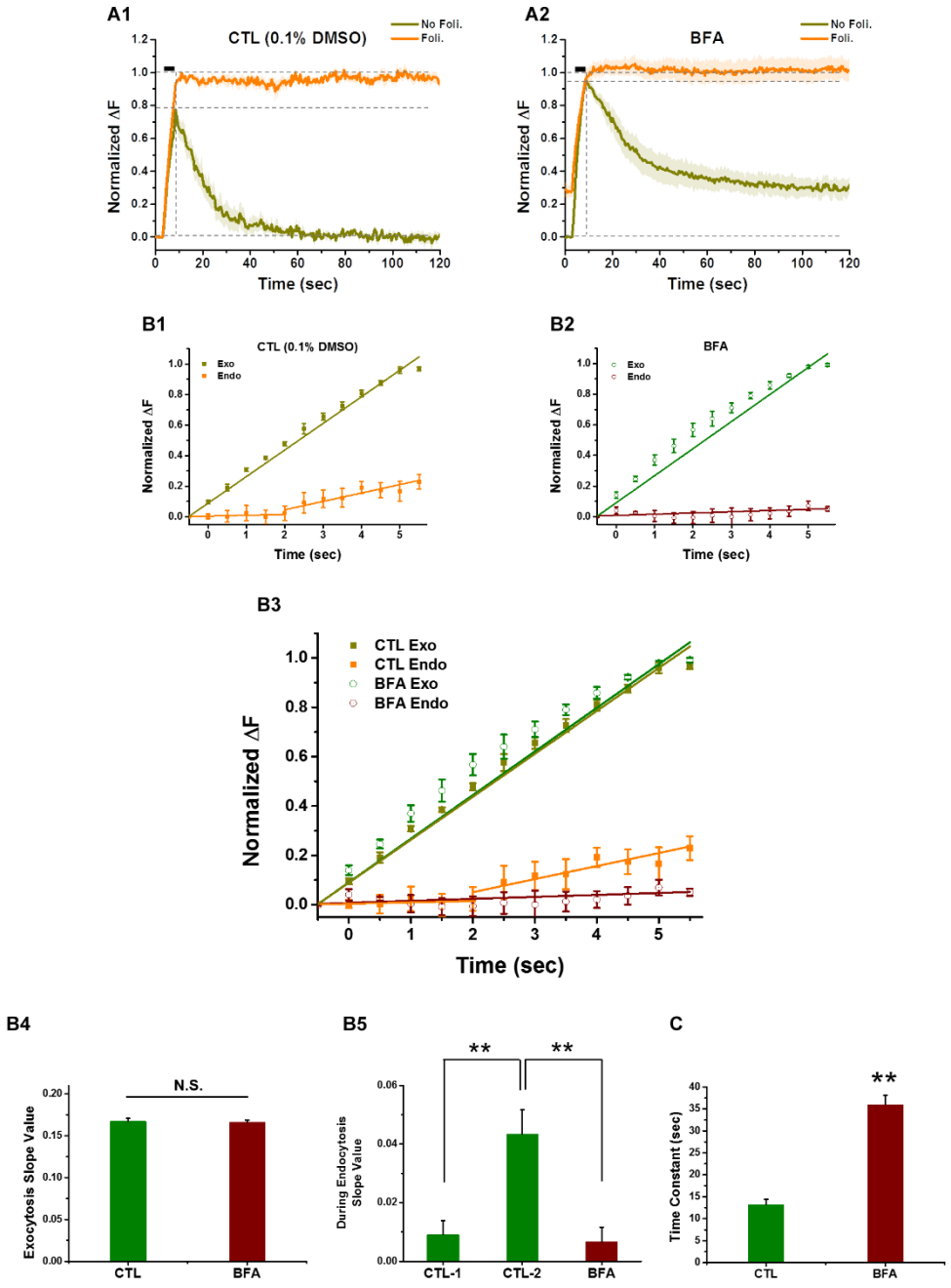
A1
CTL (0.1% DMSO)
No Foli.
Foli.
Normalized ΔF
Time (sec)
A2
BFA
B1
CTL (0.1% DMSO)
Exo
Endo
B2
BFA
B3
CTL Exo
CTL Endo
BFA Exo
BFA Endo
B4
N.S.
Exocytosis Slope Value
CTL
BFA
B5
**
**
During Endocytosis Slope Value
CTL-1
CTL-2
C
Time Constant (sec)

Figure 9. Deficiency of CIE slows endocytosis at high-frequency stimulation.

A1-A2, Average vGpH fluorescence intensity profiles of the neurons from after 30 min treatment of 0.1 % DMSO, as a control, **(A1)** or after of 10 μg/ml BFA **(A2)** with 200 APs at 40 Hz stimulation with or without *Foli*. Acute pharmacological deficiency of CIE delayed membrane retrieval induced by high-frequency stimulation, while Endocytosis induced by low-frequency stimulation was unaffected (n = 122 neurons from 5 independent coverslips for the control, n = 83 neurons from 5 independent coverslips for the BFA treated). Error bars indicate SEM.

B1-B3, Slope of the graphs are showing the time course of endocytosis (Endo) and exocytosis (Exo) during stimulation with 200 APs at 40 Hz. Rate of exocytosis and rate of endocytosis during-stimulus were obtained from the linear fits during stimulation. In the neurons applied the high-frequency stimulation, the data fitted separately at two second due to the fact that the during-stimulus endocytosis is expelled until ~ 2 s **(B1)**. Whereas, in the presence of BFA, the during-stimulus endocytosis was completely abolished during high-frequency stimulation **(B2)**. **(B3)** Those data were merged and displayed based on the time of imaging. **B4-B5,** Bar graph showed the average slope value of exocytosis **(B4)** and endocytosis **(B5)**. (exocytic rate: 0.1672 ± 0.0035 for the control, 0.1660 ± 0.0026 for the BFA treated; endocytic rate: 0.0090 ± 0.0048 for the control until ~ 2 s, 0.0439 ± 0.0082 for the control after 2 s and 0.0066 ± 0.0050 for the BFA treated). Data are presented as means ± SE. **p < 0.01(Student's *t*-test and

ANOVA with LSD post hoc test).

C, Decay of post-stimulus fluorescence of vGpH fitted by double exponential with time constant, $\tau = 13.24 \pm 1.14$ s for the control and 30.58 ± 4.69 s for the BFA treatment. Data are presented as means ± SE. **$p<0.001$ (Student's *t*-test).

Discussion

Although the pathways of endocytosis have been well noted, how particular pathway can be selected by the cell remains as an enigma. Previous studies, by using RNAi for depleting clathrin, have suggested that the majority of SVs endocytosis occurs via CME and that the SVs retrieval fraction of the fast and clathrin independent mode, such as kiss-and-run, is significantly low during the weak stimulation [11]. For neurons to maintain a high rate of firing, the retrieval and reformation of SVs must be carried out effectively [25, 26]. In addition, *clayton et al.* has proposed that bulk endocytosis is triggered only during the stimulation and the major post-stimulation retrieval pathway is CME [27]. However, recent data have challenged to these views that CME is the majority fraction of SVs endocytosis and bulk endocytosis is important only during the stimulation. In the recent study, the researchers have suggested that CME is not essential for SVs retrieval from plasma membrane under high-frequency stimulation and under this condition, the retrieval occurs via dynamin 1/3- and endophilin- dependent CIE because of limited capacity and slow speed of CME [12].

In this work, I examined how neurons choose the pathways of SVs retrieval depending on their different neuronal activity. As reported above, during low-frequency (5 Hz) stimulation, I found that SVs are retrieved from plasma membrane mostly by using CME pathway. Through the performance of exo/endocytosis assay with neurons,

whose clathrin function was defected either by knocking down endogenous CHC or acute pharmacological blockage of clathrin interaction with other accessory proteins, both during- and post-stimulus endocytic defects were detected. However, CIE blocked by depleting AP-1/3 neurons did not show any defect in SVs retrieval. Under high–frequency (40 Hz) stimulation, the clathrin inhibited-neurons normally retrieved SVs from plasma membrane but, the BFA treated-neurons, whose CIE was blocked, showed massive failing of during-stimulus endocytosis and slowdown of the post-stimulus endocytosis. These results indicated that frequency of stimulation may be one of the contributing factors that can modulate the choice of the endocytic pathways.

Previously, it has been found that activity-dependent dephosphorylation of dynamin 1 is essential molecule to trigger bulk endocytosis. Contrary to that dynamin 1 interacts with amphiphysin during CME, dephosphorylated dynamin 1 interacts with syndapin to trigger bulk endocytosis. During strong stimulation, calcium influx to the presynaptic terminals was increased and this likely had led to activate calcineurin to dephosphorylate dynamin 1 [28]. Dynamin also regulates actin dynamics [29] and deficiency of tissue-specific dynamin 1 can result in decreased short-term depression at calyx of held during high-frequency stimulation [30]. In addition, in synaptojanin knockout mice SVs endocytosis could not be recovered at intense stimulation because synaptojanin controls the levels of phosphatidylinositol (4,5) bisphosphate (PI(4,5)P2) ,which is involved in bulk endocytosis [31]. Like this, some key components of CIE have been identified recently, whereas its molecular mechanism of

modulating the endocytic pathways is still conundrum. Thus, identification molecules that could contribute to the shift between CME and CIE depending on frequency requires further study.

Moreover, in both conditions, the endocytosis during and after stimulation were not fully inhibited when one pathway was blocked. I speculated that the endocytic pathways are not necessarily restricted to one way and can compensate each other when one pathway is blocked. Because the contributing adaptor proteins are distinct between CME and CIE, this compensatory action is special in SVs pool replenishment. These results further suggest that alteration of neuronal activity can lead to more effective direction of SVs retrieval, thus contributing to synaptic plasticity.

Although the new mechanism of endocytosis, called ultrafast endocytosis, was recently proposed, this compensation is unique. The ultrafast endocytosis retrieves from plasma membrane through synaptic endosome like structure within ~ 100 ms at physiological temperature [13]. At room temperature (~22 ℃), clathrin contributes to retrieve SVs from plasma membrane rather than from synaptic endosome during applied a single stimulation. At first glance, ultrafast endocytosis seems highly relevant to this researches, however ultrafast endocytosis is known to be detected at a single or brief stimulation and reported highly temperature dependent endocytosis [14]. Thus, I exploited the physiological conditions including stimulation (5 Hz, or 40 Hz, and 200 APs) and temperature (34 ℃ ± 0.5 ℃) to figure out activity-dependent switch of

endocytosis pathways. Whether ultrafast endocytosis also functions during intense stimulation and whether temperature is also responsible for shifting from CME to CIE are certainly interesting becomes an interesting topic that requires further study.

What is physiological meaning of studying modulation of endocytosis? My results further suggest that nerve terminals utilize divergent SVs retrieval modes for adapting to their specific functions. In a previous study, bulk endocytosis has been observed only in phasic synapses but not tonic synapses at identical stimulation [32]. In addition, long-term potentiation, which contributes to memory generation, should be regulated by CIE since this event is triggered by intense tetanic stimulation. Thus, control of CIE/CME modulation may have acute effects on long-term memory [33]. Some neurological disorders can be also explained for their mechanisms by this modulation of SVs retrieval pathways. For example, activity-dependent bulk endocytosis might be essential to epilepsy, in which short burst firing occurs and brain injury is induced because of excitotoxicity [34]. Further research will provide which molecules specifically modulate SVs retrieval depending on neuronal activity in order to identify the key mechanisms of neuronal diseases.

References

1. Katz, B. and R. Miledi, *Release of acetylcholine from a nerve terminal by electric pulses of variable strength and duration.* 1965.
2. Katz, B. and R. Miledi, *Ionic requirements of synaptic transmitter release.* 1967.
3. Sudhof, T.C., *The synaptic vesicle cycle.* Annu Rev Neurosci, 2004. **27**: p. 509-47.
4. Dittman, J. and T.A. Ryan, *Molecular circuitry of endocytosis at nerve terminals.* Annual Review of Cell and Developmental, 2009. **25**: p. 133-160.
5. Doherty, G.J. and H.T. McMahon, *Mechanisms of endocytosis.* Annu Rev Biochem, 2009. **78**: p. 857-902.
6. Klingauf, J., E.T. Kavalali, and R.W. Tsien, *Kinetics and regulation of fast endocytosis at hippocampal synapses.* Nature, 1998. **394**(6693): p. 581-585.
7. Aravanis, A.M., J.L. Pyle, and R.W. Tsien, *Single synaptic vesicles fusing transiently and successively without loss of identity.* Nature, 2003. **423**(6940): p. 643-7.
8. Zhang, Q., Y. Li, and R.W. Tsien, *The dynamic control of kiss-and-run and vesicular reuse probed with single nanoparticles.* Science, 2009. **323**(5920): p. 1448-1453.
9. Koenig, J. and K. Ikeda, *Synaptic vesicles have two distinct recycling pathways.* The Journal of cell biology, 1996. **135**(3): p. 797-808.
10. Takei, K., et al., *The synaptic vesicle cycle: a single vesicle budding step involving clathrin and dynamin.* The Journal of cell biology, 1996. **133**(6): p. 1237-1250.

11. Granseth, B., et al., *Clathrin-mediated endocytosis is the dominant mechanism of vesicle retrieval at hippocampal synapses.* Neuron, 2006. **51**(6): p. 773-86.

12. Kononenko, N.L., et al., *Clathrin/AP-2 mediate synaptic vesicle reformation from endosome-like vacuoles but are not essential for membrane retrieval at central synapses.* Neuron, 2014. **82**(5): p. 981-988.

13. Watanabe, S., et al., *Ultrafast endocytosis at mouse hippocampal synapses.* Nature, 2013. **504**(7479): p. 242-247.

14. Watanabe, S., et al., *Clathrin regenerates synaptic vesicles from endosomes.* Nature, 2014. **515**(7526): p. 228-233.

15. Chang, S. and P. De Camilli, *Glutamate regulates actin-based motility in axonal filopodia.* Nat Neurosci, 2001. **4**(8): p. 787-93.

16. Lee, S., et al., *SPIN90/WISH interacts with PSD-95 and regulates dendritic spinogenesis via an N-WASP-independent mechanism.* EMBO J, 2006. **25**(20): p. 4983-95.

17. Sankaranarayanan, S., et al., *The use of pHluorins for optical measurements of presynaptic activity.* Biophysical journal, 2000. **79**(4): p. 2199-2208.

18. Kim, S.H. and T.A. Ryan, *Synaptic vesicle recycling at CNS snapses without AP-2.* J Neurosci, 2009. **29**(12): p. 3865-74.

19. von Kleist, L., et al., *Role of the clathrin terminal domain in regulating coated pit dynamics revealed by small molecule inhibition.* Cell, 2011. **146**(3): p. 471-484.

20. Dutta, D., et al., *Pitstop 2 is a potent inhibitor of clathrin-independent endocytosis.*

PloS one, 2012. **7**(9): p. e45799.

21. Nebenführ, A., C. Ritzenthaler, and D.G. Robinson, *Brefeldin A: deciphering an enigmatic inhibitor of secretion.* Plant physiology, 2002. **130**(3): p. 1102-1108.

22. Cheung, G. and M.A. Cousin, *Adaptor protein complexes 1 and 3 are essential for generation of synaptic vesicles from activity-dependent bulk endosomes.* J Neurosci, 2012. **32**(17): p. 6014-23.

23. Voglmaier, S.M., et al., *Distinct endocytic pathways control the rate and extent of synaptic vesicle protein recycling.* Neuron, 2006. **51**(1): p. 71-84.

24. Blumstein, J., et al., *The neuronal form of adaptor protein-3 is required for synaptic vesicle formation from endosomes.* J Neurosci, 2001. **21**(20): p. 8034-42.

25. Royle, S.J. and L. Lagnado, *Endocytosis at the synaptic terminal.* The Journal of physiology, 2003. **553**(2): p. 345-355.

26. Rizzoli, S.O. and W.J. Betz, *Synaptic vesicle pools.* Nat Rev Neurosci, 2005. **6**(1): p. 57-69.

27. Clayton, E.L., G.J. Evans, and M.A. Cousin, *Bulk synaptic vesicle endocytosis is rapidly triggered during strong stimulation.* J Neurosci, 2008. **28**(26): p. 6627-32.

28. Armbruster, M., et al., *Dynamin phosphorylation controls optimization of endocytosis for brief action potential bursts.* Elife, 2013. **2**: p. e00845.

29. Orth, J.D. and M.A. McNiven, *Dynamin at the actin–membrane interface.* Current opinion in cell biology, 2003. **15**(1): p. 31-39.

30. Mahapatra, S., F. Fan, and X. Lou, *Tissue-specific dynamin-1 deletion at the calyx*

of Held decreases short-term depression through a mechanism distinct from vesicle resupply. Proceedings of the National Academy of Sciences, 2016: p. 201520937.

31. Mani, M., et al., *The dual phosphatase activity of synaptojanin1 is required for both efficient synaptic vesicle endocytosis and reavailability at nerve terminals.* Neuron, 2007. **56**(6): p. 1004-18.

32. Evergren, E., et al., *Differential efficiency of the endocytic machinery in tonic and phasic synapses.* Neuroscience, 2006. **141**(1): p. 123-131.

33. Clayton, E.L. and M.A. Cousin, *The molecular physiology of activity-dependent bulk endocytosis of synaptic vesicles.* Journal of neurochemistry, 2009. **111**(4): p. 901-914.

34. Richards, D., C. Guatimosim, and W. Betz, *Two endocytic recycling routes selectively fill two vesicle pools in frog motor nerve terminals.* Neuron, 2000. **27**(3): p. 551-559.

Abstract in Korean (국문 초록)

전형적인 중추신경계의 시냅스는 한정된 개수의 시냅스낭을 함유하고 있다. 반복적인 자극에 대응하여 계속적으로 신경 전달 물질을 분비할 수 있으려면 세포 내 함입 과정과 시냅스낭 재생성 및 순환 과정을 통해 신경 전달 물질을 함유한 시냅스낭이 빠르게 보충되어야 한다. 이러한 시냅스낭의 이입 과정은 clathrin-mediated endocytosis (CME) 과정이 독점적으로 관여한다는 보고가 있었으나, 최근 ultrafast endocytosis 나 bulk endocytosis 와 같은 clathrin-independent endocytosis (CIE) 과정이 더 우세하게 작용한다는 것이 보고된 바 있다. 그러나 신경 세포가 신경 활성 상태에 따른 CME 과정과 CIE 과정에 대하여 어떤 방법을 이용하여 시냅스낭 이입 과정을 일으키는지에 관해서는 아직 연구된 바가 없다. 본 연구에서는 초대 배양한 해마 신경 세포를 저주파 (5 Hz) 와 고주파 (40 Hz) 로 나누어 자극을 주어 신경 활성 상태에 따른 시냅스낭 이입 과정이 어떻게 조절되는지 확인하는 실험을 진행하였다. 5 Hz 와 같은 저주파의 자극이 들어가는 동안에는 오로지 CME 과정을 통한 시냅스낭 이입 과정만이 일어난다는 것을 확인하였다. 이는 Brefeldin A (BFA) 를 처리하거나 adaptor protein (AP) -1/ -3를 knockdown 시킴으로써 CIE 과정을 저해하였을 때, 5 Hz 자극이 들어가는 동안에, 어떠한 시냅스낭 순환 과정의 저해를 보이지 않았다는 것을 통해 이를 증명하였다. 그러나, PITSTOP 2 를 처리하거나 clathrin heavy chain (CHC) 을 knockdown 시킴으로써 CME 과정을

저해했을 때는, 자극이 들어가는 초기 (약 10 초까지) 의 시냅스낭 이입이 차단되다가 이후 CME 과정의 결핍을 보상하기 위해 CIE 과정을 통하여 시냅스낭 이입 과정을 재개한다는 것을 확인하였다. 또한 자극이 끝난 이후의 시냅스낭 이입은 CIE 과정의 저해는 영향을 주지 않지만, CME 과정의 저해는 이입 과정의 속도를 느리게 만든다는 것을 확인하였다. 위 결과와 반대로, 40 Hz와 같은 고주파 자극이 들어가는 동안에 일어나는 시냅스낭 이입 과정은 약간의 지연 이후에 CIE 과정이 중점적으로 일어난다는 것을 확인하였다. 이는 CME 과정을 저해 시켰을 때는 아무런 영향이 없었던 것과 달리 CIE 과정을 저해 시켰을 때 시냅스낭 이입 과정이 완전히 차단된다는 것을 통해 증명하였다. 또한 자극이 끝난 후의 이입 과정도 CME 과정의 저해는 영향을 주지 않으나, CIE 과정이 저해되면 현저히 느리게 일어난다는 것을 확인하였다. 위 결과를 토대로, 자극이 들어가는 동안에 성숙한 신경세포가 신경 활성에 기반하여 CME 과정과 CIE 과정을 다르게 사용한다는 것을 증명하였다. 또한 한쪽 방법이 저해되면 다른 방법을 재개하여 이러한 결핍을 보상한다는 것을 확인하였다. 위 연구를 통해 신경세포가 활성 상태에 따른 시냅스낭 이입 방법의 효율적인 변화와 보상작용을 확인했다는 것을 고려해 볼 때, 이러한 연구 결과는 궁극적으로 신경 전달 물질 방출과 시냅스 가소성 연구에 이바지 할 것을 제시한다.

주요어 : 신경활성상태, 클라트린 매개 세포 내 이입, 클라트린 비 의존성 세포 내 이입, 시냅스낭 순환 과정, 활성 의존적 조절

학 번 : 2014-22453